Colloid Polym Sci (2006) 284: 965–978
DOI 10.1007/s00396-005-1383-5

ORIGINAL CONTRIBUTION

F. Sayar
G. Güven
E. Pişkin

Magnetically loaded poly(methyl methacrylate-*co*-acrylic acid) nano-particles

Received: 8 April 2005
Accepted: 7 July 2005
Published online: 15 September 2005

F. Sayar · G. Güven · E. Pişkin (✉)
Department of Chemical Engineering
and TÜBİTAK-Biyomedtek
Center for Biomedical
Technologies Beytepe,
Hacettepe University,
Ankara 06800, Turkey
E-mail: piskin@hacettepe.edu.tr

Abstract Magnetically loaded polymeric nano-particles carrying functional groups on their surface were prepared by a two-stage process. In the first stage, super-paramagnetic magnetite (Fe_3O_4) nano-particles were produced by a co-precipitation method from the aqueous solutions of $FeCl_2{\cdot}4H_2O$ and $FeCl_3{\cdot}6H_2O$ using a NaOH solution. The smallest size obtained was 40.9 nm with polydispersity index of 0.194 obtained by using a Zeta Sizer. The effects of Fe^{2+}/Fe^{3+} molar ratio, stirring rate, temperature, base concentration, and pH on the particle size/size distribution and stability of the dispersions were examined. Increasing the relative concentration of Fe^{2+} ion and decreasing the stirring rate and pH increased the particle size, while the concentration of NaOH and temperature did not change the particle size significantly. Polymer coating was achieved by emulsion polymerization at high surfactant to monomer ratio of methyl methacrylate (MMA) and acrylic acid which were used as comonomers (comonomer ratio: 90/10 weight) with high surfactant to monomer ratio. The surfactant and initiator were SDS and KPS, respectively. Nano-particles in the range of 115 and 300 nm in diameter were produced depending on recipe. Increasing the Fe_3O_4/monomer and surfactant/monomer ratios, the KPS concentration caused a decrease in the average diameter. Magnetic properties of the nano-particles were obtained by electron spin resonance and vibrating-sample magnetometer. Most of the polymer-coated nano-particles exhibited super paramagnetic behavior.

Keywords Magnetite nano-particles · Poly(methyl methacrylate-co-acrylic acid) · Magnetically loaded polymeric nano-particles · Emulsion polymerization

Introduction

Magnetic colloidal nano-particles are increasingly used in bio-separation, in biosensor, and in diagnosis and therapy in medicine including immunoassays, medical imaging and targeted drug delivery [1–5]. Several kind of magnetic polymer nano-particles, which are usually dispersed in a carrier liquid (usually water), therefore called also as ''latex'', with tailor-made properties depending on the final application have been produced from both natural and synthetic polymers [2, 6–10]. Here, magnetic seed nano-particles (Fe_3O_4) are coated with a polymeric layer. Polymer coating prevents the direct interaction of inorganic magnetic materials with the biological system and therefore reduces toxicity and further increases biocompatibility of the nano-particles, and also create functional groups (coming from the polymer chemical structure) on the surfaces of the nano-particles which would be available for modifications for specific applications. In addition to their biocompatibility, magnetic polymer nano-particles should fulfill some criteria to fit further biomedical applications: no

sedimentation (stable latexes), uniform size and size distribution, high and uniform magnetic content, superparamagnetic behavior, no toxicity, no metal-ions (e.g., iron) leakage, etc.

Much attention has been paid to the preparation of different kinds of magnetic polymeric particles in the past decades and various strategies have been performed producing magnetic polymeric particles. Encapsulation of magnetic particles with preformed natural or synthetic polymers is the simple and classical method to prepare magnetic polymeric particles, but the particle size and shape prepared by this method are random. In order to control the shape and structure of the magnetic polymeric particles, Ugelstad et al. [8] developed an effective method through direct precipitation of iron salt inside the porous polystyrene particles. The development of emulsion polymerization, such as the conventional micro-emulsion polymerization, soap-free emulsion polymerization, mini-emulsion polymerization and micro-emulsion polymerization, has led to new synthesis methods [2, 6, 7, 11, 12]. The typical method based on emulsion polymerization is to suspend magnetic particles in the dispersed phase and then polymerize the monomer in the presence of the magnetic particles to form magnetic polymeric particles. Considering the mechanism of different emulsion polymerizations, the mini-emulsion polymerization is very suitable for making magnetic polymeric particles. In mini-emulsion polymerization, the monomer droplets with magnetic nano-particles act as "nano-reactors", the magnetic polymeric particles can be prepared in situ. Recently, Ramirez et al. [2] used a new three-step preparation route including two mini-emulsion processes to encapsulate magnetic particles by polystyrene successfully, Wormuth [11] achieved 140–220 nm magnetic polymeric particles using monomers (2-hdroxyethylmethacrylate and methacrylic acid) and a diblock polymer emulsifier (poly(ethylene-co-butylene)-*b*-poly(ethylene oxide)), via inverse mini-emulsion polymerization. Polymethacrylate/poly(hydroxymethacrylate)-coated magnetite particles could be also prepared by a single inverse microemulsion process, leading to particles with a narrow size distribution, but only with a magnetite content of 3.3 wt% [7]. Magnetite-containing nano-particles of 150–200 nm were also synthesized by seed precipitation polymerization of methacrylic acid and hydroxyethyl methacrylate in the presence of magnetite particles containing tris(hydroxymethyl)aminomethane hydroxide in ethyl acetate medium [13].

There are several different synthetic methods to form magnetite nano-particles. Synthetically, magnetite is formed by two fundamental processes: size reduction and aqueous precipitation. Ball mill grinding micrometer-sized magnetite powder was one of the first methods, developed by Papell in the late 1960 s. Long grinding periods of 500–1,000 h are required to form the nano-particles, and therefore this method has been essentially replaced by aqueous precipitation methods. Aqueous methods for magnetite nano-particle formation include: oxidation of Fe^{2+}; formation in water-in-oil microemulsion, vesicles, apoferritin; liposomes; and in the presence of polymers. However, the most common synthetic route to magnetite is the co-precipitation of hydrated divalent and trivalent iron salts in the presence of a strong base. This process is more feasible to apply in the production of more homogeneous magnetite particles. This method results in the synthesis of a precipitate, which needs ulterior processing (centrifugation, washing and magnetic separation) before re-dispersion in water and eventually an ulterior coating. Magnetite particles may also be synthesized at high temperature or by hydrolysis and oxidation of $Fe(OH)_2$ suspensions at elevated temperatures. The majority of wet processes give rise to products with a good crystallinity and magnetization, but with bigger particles [14]. Recently magnetite nano-particles were synthesized by precipitation with forced mixing in aqueous solution without any surfactants. The method of the forced mixing has an advantage of controlling a high product saturation degree and a constant pH value of the reaction system during the forced mixing process, which causes to form particles with a small size and a narrow size distribution [15].

In this study, magnetically loaded polymeric nano-particles carrying functional group on their surface were prepared by a two-stage process. First, magnetite (Fe_3O_4) nano-particles were produced by an aqueous phase co-precipitation method. The effect of Fe^{2+}/Fe^{3+} molar ratio, stirring rate, temperature, pH, base concentration on the particle size, and size distribution of magnetite nano-particles were examined. Then these nano-particles were coated with a polymeric layer by copolymerization of methyl methacrylate (MMA) and acrylic acid in an emulsion at a high surfactant to monomer ratio. The effect of the type of the initiator and surfactant, the concentration of the initiator, the magnetite/monomer ratio and surfactant/ monomer ratio on the particle size and size distribution were examined.

Materials and methods

Materials

Ferric chloride hexahydrate ($FeCl_3 \cdot 6H_2O$, 99%) and ferrous chloride tetrahydrate ($FeCl_2 \cdot 4H_2O$, 99%), tetramethylammonium hydroxide (TMAOH) and sodium hydroxide (NaOH) were purchased from Sigma (Taufkirchen, Germany) and used as received. Sodium dodecyl sulfate (SDS), cetyltrimethylammonium bromide (CTAB), dodecyl-trimethylammonium bromide (DTAB), potassium persulfate (KPS), 2,2′-az-

obis(isobutyronitrile) (AIBN), 2,2′-azobis(2-amidinopropane) dihydrochloride (V_{50}) and sulfuric acid (98%) were obtained from Aldrich (Taufkirchen,Germany) and used as received. The main monomer MMA was purchased from Fluka (Taufkirchen, Germany) and was treated with an aqueous solution of NaOH (10%) to remove the inhibitor before use. Acrylic acid (AAc) was also obtained from Fluka but used without any pretreatment.

Synthesis of magnetite (Fe_3O_4) nano-particles

The magnetite nano-particles were produced by co-precipitation of Fe^{2+} and Fe^{3+} from their aqueous solutions using NaOH as originally reported by Zhu et al. [15]. Our attempt was to optimize the reaction conditions to synthesize magnetite particles that are around 50 nm or even smaller. In order to reach this task we have conducted a series of preliminary experiments in which we were able to decide the type of the parameter which would effective the size and stability of the magnetite nano-particles, and their ranges to be changed. Then we designed the experiments given in Table 1 in which we changed Fe^{2+}/Fe^{3+} mole ratio, stirring rate, temperature, precipitation agent (NaOH) concentration, and pH. Note that in order to increase the stability of the dispersions containing magnetite nano-particles we introduced low polarizing positively charged ions, i.e., $N(CH_3)_4^+$ ion of tetramethylammonium hydroxide (TMAOH) as suggested by Massart [16].

In a typical procedure, a 120 ml aqueous solution containing Fe^{2+} and Fe^{3+} salts (total 1.25 M) and 120 ml of 5 M NaOH solution were added into the reactor containing 160 ml distilled water at 80 °C under N_2 atmosphere, by vigorous agitation. The black precipitate was formed at the early phase, but the medium was continuously stirred for 2 h at a given stirring rate and temperature followed by the slow addition of 10 ml 25% (w/w) TMAOH to stabilize the magnetite particles.

Synthesis of magnetic polymeric nano-particles

The magnetite nano-particles produced with a recipe M1 (see Table 1) with an average particle size of 40.9 nm with a particle size distribution (as polydispersity index, PDI) of 0.194 were selected as the most suitable size for further studies, and used in the second step, in which they were coated with acrylic polymers containing carboxylic acid functional groups (coming from the comonomer acrylic acid, AAc). Polymer coating was achieved by emulsion polymerization at a high surfactant to monomer ratio conducted in an oil-in-water (o/w) system.

Several parameters, including the magnetite nano-particles/monomer ratio, type of the surfactant (SDS, CTAB, DTAB), the type and the amount of the initiator (water-soluble KPS, oil-soluble AIBN, cationic V-50), monomer/surfactant weight ratio, were changed in different ranges as given in the recipes in Table 2, and the particle size and size distributions (PDI) were obtained. MMA and AAc were used as comonomers with a weight ratio of 90/10. The surfactant and monomer concentrations were 9.33 and 6.34% wt, respectively.

In a typical polymerization procedure, surfactant was added to the magnetite suspension previously synthesized (2% wt) in a 100 ml pyrex reactor. Then, the

Table 1 Co-precipitation recipe for production of magnetite nano-particles[a]

Experiment no.	Fe^{2+}/Fe^{3+} ratio (mol/mol)	Stirring rate (rpm)	Temperature (°C)	NaOH conc. (M)	pH
M1	**0.5**	3,000	80	5	12
M2	**1.0**	3,000	80	5	12
M3	**1.5**	3,000	80	5	12
M4	**2.0**	3,000	80	5	12
M5	0.5	**1,000**	80	5	12
M6	0.5	**1,500**	80	5	12
M7	0.5	**2,000**	80	5	12
M8	0.5	**3,000**	80	5	12
M9	0.5	2,000	**20**	5	12
M10	0.5	2,000	**40**	5	12
M11	0.5	2,000	**60**	5	12
M12	0.5	2,000	**80**	5	12
M13	0.5	2,000	80	**2.5**	12
M14	0.5	2,000	80	**5.0**	12
M15	0.5	2,000	80	**7.5**	12
M16	0.5	2,000	80	**10.0**	12
M17	0.5	2,000	80	5	**3**
M18	0.5	2,000	80	5	**6**
M19	0.5	2,000	80	5	**9**
M20	0.5	2,000	80	5	**12**

[a]The reaction (stirring) time was 2 h in all these experiments.

comonomer mixture was added to this dispersion which was mixing in an ultrasonic bath for about half an hour in order to ensure dispersion of the magnetite nano-particles and the monomers. Prior to polymerization, initiator was added to the solution and nitrogen gas blown through the medium for about 1–2 min to remove dissolved oxygen. Polymerizations were carried out in a constant temperature shaking bath at 65 °C, under nitrogen atmosphere for 24 h. After the polymerization, the magnetic polymeric nano-particles were cleaned by washing with methanol and water several times to remove the surfactant and the unreacted monomers. The magnetic nano-particles were collected with the help of a magnet and washed with distilled water several times. Then these particles were immersed in 0.1 M of H_2SO_4 solution for 48 h to separate the magnetite nano-particles, which were not coated (naked) with a polymer layer. After that polymer-coated particles were further washed with deionized water.

Characterization

The average particle size, size distributions, and surface charges were determined by Zeta Sizer (Malvern Instruments, Model 3000 HSA, France).

The crystalline structure and particle sizes were investigated with powder X-ray diffractometer (XRD, Rigaku RU-200, Japan). The XRD patterns were taken from 10 to 80 (2θ value) using Cu Kα radiation at room temperature. The XRD graphics were compared to the ASTM XRD graphics in order to deduce the crystal structure of the product.

FTIR spectra of the polymer-coated nano-particles were obtained by using an FTIR spectrophotometer (Shimadzu, Model: FTIR-8000 series) with KBr (IR grade)–nano-particle mixture in the powder form.

Thermal transitions were obtained by using a differential scanning calorimeter (DSC) (Shimadzu, Model DSC-50, Japan). Nitrogen was used as the sweeping gas. The samples (5–10 mg) were heated at a scan rate of 10 °C min^{-1} from 25 °C to 500 °C followed by rapid cooling.

TGA thermograms were also obtained by thermogravimetric analysis (TGA) (Setaram, Labsys, France). About 10 mg sample was placed into aluminia crucible with increasing temperature (10 °C min^{-1}) in a controlled, flowing air atmosphere, and heated from 25 °C to 550 °C.

Electron spin resonance (ESR) spectra of the magnetite nano-particles and their polymer-coated forms transferred into sealed tubes of 4 mm internal diameter were recorded using a Varian E-line 9 spectrometer (Germany) with TE_{102} type double cavity resonator. ESR spectra of the samples were displayed in the form of the first derivative of the absorption peak plotted against magnetic field. All measurements were made at room temperature. Spectrometer operating conditions are 9.3 GHz, 3,300 field set, 100 Hz field modulation, 1 G peak-to-peak modulation amplitude and 1 mW microwave power to determine signal intensities, line widths, and *g*-values. All ESR signal intensities were performed using a DPPH standard sample.

Magnetic properties of magnetite nanoparticles and their polymer-coated forms were determined using PAR-150A parallel field vibrating sample magnetometer (USA) in conjunction with a Fieldial Mark II Varian (Germany) electromagnet assembly that can provide a maximum magnetic field of 2.0 T. The sample was

Table 2 Emulsion polymerization recipe[a]

Experiment no.	Surfactant type	Initiator type	Conc. (mM)	Magnetite/monomer ratio (wt%)	Surfactant/monomer ratio (wt/wt)
P1	**SDS**	KPS	1.5	25	1.47
P2	**CTAB**	KPS	1.5	25	1.47
P3	**DTAB**	KPS	1.5	25	1.47
P4	SDS	**KPS**	1.5	25	1.47
P5	SDS	**AIBN**	1.5	25	1.47
P6	SDS	**V-50**	1.5	25	1.47
P7	SDS	KPS	**1.5**	25	1.47
P8	SDS	KPS	**2.0**	25	1.47
P9	SDS	KPS	**2.5**	25	1.47
P10	SDS	KPS	1.5	**5**	1.47
P11	SDS	KPS	1.5	**25**	1.47
P12	SDS	KPS	1.5	**50**	1.47
P13	SDS	KPS	1.5	25	**1.11**
P14	SDS	KPS	1.5	25	**1.47**
P15	SDS	KPS	1.5	25	**2.94**

[a]The monomer concentration, polymerization temperature, and polymerization time were 6.34% wt, 65°C, and 24 h, respectively, in all these experiments.

placed into magnetic field vibrating with a constant frequency. Magnetic fields of 0–2.0 T were applied to the samples for the determination of magnetization. The magnetic properties of the particles were expressed in electron mass units (emu).

Results and discussion

In this study, we attempted to prepare "magnetic polymeric nano-particles", or in other terms "polymer-coated magnetite nano-particles" which are carrying functional group on their surfaces for further treatments and therefore related applications. A two-step process was applied in which; first, Fe_3O_4 ("magnetite") super paramagnetic particles were prepared by an aqueous phase co-precipitation, and then these nano-particles were coated with a polymer layer containing functional groups by emulsion polymerization at a high surfactant to monomer ratio. In both the steps, our main aim was to find out the effects of several parameters on particle size and size distribution, and of course to reach long-term stable latexes. The results of these two groups (steps) of studies are given and discussed below separately.

Magnetite nano-particles

Particle size and size distribution of magnetite nano-particles

The average particle size and size distribution of the magnetite nano-particles prepared in the first step were measured by Zeta Sizer. Table 3 gives these values obtained at different conditions. Note that in each group only one parameter was changed (given in bold in Table 3) the others were the same (see Table 1 for recipe). The average particle size was an average of minimum 30 measurements, and the size distributions (or the so-called PDI) were recorded automatically by the software of these repeated measurements.

Effects of Fe^{2+}/Fe^{3+} mole ratio

In this study, Fe^{2+}/Fe^{3+} ratio in the initial mixture was selected as one of the parameters, which is effective on the particle size of magnetite nano-particles to be produced by co-precipitation following the statements given in the related literature [15–17]. The chemical reaction of magnetite precipitation is expected as follows:

Table 3 Effects of several parameters on particle size and size distribution of magnetite nano-particle[a]

Experiment no.		Average particle size (nm)	Particle size distribution (PDI)
Fe^{2+}/Fe^{3+} ratio (mol/mol)			
M1	**0.5**	40.9	0.194
M2	**1.0**	91.6	0.326
M3	**1.5**	112.3	0.308
M4	**2.0**	130.0	0.577
Stirring rate (rpm)			
M5	**1,000**	325.6	0.637
M6	**1,500**	224.9	0.414
M7	**2,000**	130.7	0.517
M8	**3,000**	61.9	0.256
Temperature (°C)			
M9	**20**	130	0.234
M10	**40**	136.7	0.294
M11	**60**	145	0.326
M12	**80**	150.2	0.341
NaOH Conc. (M)			
M13	**2.5**	148.5	0.520
M14	**5.0**	143	0.324
M15	**7.5**	138.2	0.317
M16	**10.0**	134.9	0.414
pH			
M17	**3**	391	0.167
M18	**6**	274.7	0.153
M19	**9**	217.4	0.362
M20	**12**	134	0.335

[a]The reaction conditions in each experimental group are given in Table 1.

$$Fe^{2+} + 2Fe^{3+} + 8OH^- \rightarrow Fe_3O_4 + 4H_2O \quad (1)$$

It means that the co-precipitation reaction requires 1 mol of Fe^{2+} ions and 2 mol of Fe^{3+} ions (or an Fe^{2+}/Fe^{3+} ratio of 0.5) for stoichiometric conversion. However, the Fe^{2+} salts are oxidatively unstable, and are oxidized to akaganite forms (FeOOH), as indicated by color change in the medium. Storing the reagents under nitrogen and careful deoxygenation of all solutions prior to use are pre-requirements to increase the stability and therefore to prevent these undesirable changes. It is also recommended that the mixture should be prepared freshly under nitrogen atmosphere just before the co-precipitation procedure and used immediately to prevent oxidation or other side reactions. Note that addition of base for co-precipitation should be also rapid (1–2 s) with intense agitation. A slow base addition not only causes formation of the oxidation but also may create homogeneous regions of the hydrated ion species, in which leads to nonmagnetic iron compounds.

Therefore, oxidative instability of the Fe^{2+} ion has led some researchers to the use of molar ratio of Fe^{2+}/Fe^{3+} larger than 0.5 [17, 18]. However, as also stated in the related literature, the following reactions may occur when there is excess of Fe^{2+} ions in the medium by addition of base for precipitation. The $Fe(OH)_2$ formed is converted to ferric oxide, which then slowly produces ferric (Fe^{3+}) ions that interact with ferrous compounds to yield magnetite usually with larger size [15].

$$Fe^{2+} + NaOH \rightarrow Fe(OH)_2 \quad (2)$$

$$Fe(OH)_2 \rightarrow \text{“green rust”} \rightarrow Fe_3O_4 \quad (3)$$

Following these statements given in the literature, we also change the Fe^{2+}/Fe^{3+} ratio between 0.5 and 2. Note that it was not possible to produce magnetite latexes stable enough if the ratio was lower than 0.5. The smallest size obtained was 40.9 nm (the sample M1) with PDI of 0.194 in which the Fe^{2+}/Fe^{3+} ratio was 0.5. It should carefully be noted that co-precipitation results in magnetite nano-particles mostly around 8–12 nm. Therefore, most likely the nano-particles (even those smallest ones) contain a number of magnetite primary particles, in other words there are aggregates.

When we increased the relative concentration of Fe^{2+} ions in the solution, the particle size also increased, most probably due to side reactions mentioned above. Note that in the preliminary studies even at these conditions the particle sizes were quite large and size distribution was broad. In some recipe the nano-particles were nonmagnetic, and latexes were not stable. We were able to prevent these undesirable events only with properly deoxygenated solutions, working under nitrogen atmosphere, and applying very rapid base addition with extensive agitation.

Effects of stirring rate

In this part of the study, effect of stirring rate was examined on the basis of related literature [19]. Morais et al. [19] reported the effect of stirring rate on the size of cobalt ferrite nano-particles. They synthesized cobalt ferrite nano-particles by using different stirring range in the range 2,700–8,100 rpm by co-precipitation method. It was found that increasing the stirring speed from 2,700 to 8,100 rpm reduces the average particle diameter from 15.1 to 11.4 nm. Following this information, in our studies we changed the stirring rate in the range of 1,000–3,000 rpm. Smaller particles were produced at higher stirring rates as expected. The average particle size reduced very significantly, from 325.6 to 61.9 nm by increasing the stirring rate from 1,000 to 3,000 rpm. The narrowest particle size distribution was observed with the smallest particles which synthesized with the highest stirring rate (Table 3).

The decrease of the particle size as the stirring rate increases may indicate that the nano-particle growth process is mainly dominated by the nano-particle diffusion throughout the medium instead of the diffusion of the aqueous cations into the particle surface. As the stirring rate increases, the time the nano-particle speed during a sequence of short flies also increases, allowing the onset of a higher density of nucleation sites, with consequent reduction of the particle size [19].

Effects of temperature

In the related literature it was pointed out that the preparation temperature has an important effect on the properties of the Fe_3O_4 particles [20, 21]. They reported that it is necessary to work at high temperatures to reach optimal crystal growth and particle formation. The preparation temperature, not only alters the particle size but also the morphology of Fe_3O_4 from spherical to cubic. With increasing preparation temperature the grains grow rapidly, with different growth rates for the different crystal planes that result in the changes in the shape of the products. They suggested also that the temperature of formation should not exceed 353 K, where the quality of the particle is affected negatively.

Considering previous reports in the related literature, in this study magnetite nano-particles were synthesized at four different temperatures, 20 °C, 40 °C, 60 °C, and 80 °C. Table 3 shows the particle size and size distribution for the Fe_3O_4 nano-particles, which was prepared at observable (but not very significant) particle size increases were noted when the reaction temperature was

increased. The maximum particle size (150.2 nm) was achieved at 80 °C, while the particle size distribution was broader (0.341) than those observed at lower temperatures (the sample M12 in Table 3).

Effects of NaOH concentration

Several bases including KOH, NaOH, LiOH, and NH_4OH have been used in the production of magnetite nano-particles by co-precipitation method, and suggested that the type and concentration of the base affects both the size and magnetic properties of the magnetite particles [20, 22–24]. Kim and coworkers synthesized the magnetite nano-particles under different conditions by co-precipitation, and reported that when the concentration of precipitating NaOH solution was increased from 0.9 to 1.5 M at pH 14, the particle size was increased from 13 to 30 Å [22]. Gribanov et al. showed that the saturation magnetization increased in order of the following base strengths: KOH > NaOH > LiOH > NH_4OH in the co-precipitation of magnetite nano-particles [20]. Babes et al. formed magnetite nano-particles using NH_4OH with different concentrations from 0.25 to 2.0 M and suggested that there were no significant effects on the magnetic properties of the particles [23].

After preliminary studies, as suggested by Jiang et al. [24], we decided to use NaOH as the co-precipitation agent. As seen in Table 3, with the change in the NaOH concentration in a wide range (from 2.5 to 10 M), we did not observe a decrease in the size but not very significantly, which was around 135–140 nm. The PDI value of magnetite nano-particle obtained by co-precipitation using NaOH with different concentrations were in the range of 0.324–0.520.

Effects of pH

The pH value of the solution for precipitation plays an important role in controlling the particle size and magnetic properties [25, 26]. According to Eq. 1 given above, a complete precipitation of Fe_3O_4 should be expected between pH 7–14 while maintaining a molar ratio of $Fe^{2+}/Fe^{3+} = 0.5$ under a nonoxidizing environment. Nonmagnetic iron oxyhydroxides (e.g., Goethite, Lepidocrocite) were synthesized at very high or low pHs [25]. It was proposed that pH values should be higher than 7 to produce magnetite nano-particles. It was also reported that stability of ferro-fluid depends on pH. Below pH 7 ferro-fluids become unstable, and resulting in faster sedimentation as the pH is decreased.

In order to observe the effects of pH on co-precipitation and product stability, we also studied both below (3–6) and above (9–12) neutral pH. As seen in Table 3 (and also Fig. 1), increase in the pH from 3 to 12 has resulted in a significant decrease in particle size from 391 (M17) to 134 nm (M20), and a significant increase in PDI from 0.167 to 0.362.

In this group of experiments we measured also zeta potentials of the magnetite nano-particles produced. The zeta potentials dropped significantly when the pH was increased, in parallel to the decrease in particle size. Positive values were observed in acidic region, however, zeta potentials were negative above pH 7, as also reported by Cornell and Schertmann [26]. Note also that nano-particles produced below pH 7 were not stable and exhibit magnetic properties.

Properties of magnetite nano-particles

FTIR spectra of magnetite (Fe_3O_4) nano-particle were obtained. Two typical bands at 678.2 and 408 cm^{-1} were

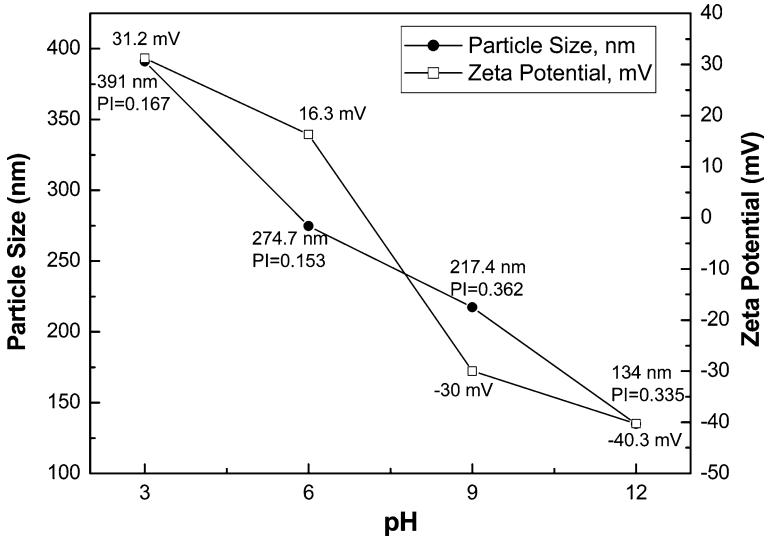

Fig. 1 Effects of pH on particle size and size distribution and zeta potentials of nano-particles produced

observable, which correspond to the stretching vibration of Fe–O group of magnetite nano-particles observed as also stated in the related literature [1, 27, 28].

Crystallographic structure of the magnetite particle was analyzed from XRD patterns [28]. Experimental *d* spacings obtained from these patterns are given in Table 4. Note that the XRD graph of the magnetite nano-particles produced in this study were very similar to the ASTM XRD graphics of Fe_3O_4, which exhibit the same inverse spinal structure. XRD results exhibited that the iron oxide particles are composed of magnetite (Fe_3O_4).

Thermal behavior of the magnetite was examined by DSC. From the DSC thermograms we observed that the physically adsorbed water leaves the structure at 71.5 °C. The broad exothermic transition at 193.87 °C was attributed to the magnetite (Fe_3O_4) to maghemite (γ-Fe_2O_3) transition. It is reported that temperatures greater than 300 °C magnetite (Fe_3O_4) is oxidized to hematite (α-Fe_2O_3) [29]. Therefore, a sharp exothermic peak was observed at 308.7 °C which shows the maghemite to hematite transition.

Magnetic polymeric nano-particles

Particle size and size distribution

In this second step, for production of magnetic polymeric nano-particles, the magnetite (Fe_3O_4) nano-particles with an average size of 40.9 nm synthesized in the previous step (see Table 3) were used as seed particles. A series of magnetic polymeric particles (called here as "poly(MMA/AAc-90/10)"copolymers) were prepared by emulsion polymerization of comonomers at a high surfactant to monomer ratio, i.e., MMA and AAc at different experimental conditions. The comonomer ratio, MMA/AAc was 90/10 in all cases. Note that it was not possible to produce emulsions when the AAc initial content was more than 10%, also according to our pervious expertise [30]. In order to ensure the polymer coating these magnetic polymeric nano-particles were titrated with 0.05 N NaOH to determine the COOH groups on the particle surface. Calculated number of moles of COOH groups is found as 1.2 mmol g^{-1} polymer (for the particles in P4, see Table 2). We changed the following parameters and investigated their effects on mainly polymeric particle size and its distribution: surfactant and initiator type, magnetite (Fe_3O_4)/monomer ratio, surfactant (SDS)/monomer ratio, and initiator (KPS) concentration. The findings and discussion are given below in the separate subsections.

Table 4 Summary data of experimental *d* (exp) (Å) spacing obtained from the X-ray patterns and from ASTM data cards [8] for iron oxide (*d* (Fe_3O_4))

2θ (exp)	*d* (exp)	*d* (Fe_3O_4)
17.460	5.07	4.852
30.200	2.96	2.099
56.720	1.62	1.615
62.500	1.48	1.484

Effects of surfactant and initiator type

In this section magnetic poly(MMA/AAc-90/10) copolymeric nanoparticles were produced by using different type of surfactants (i.e., SDS, CTAB, and DTAB) and/or initiators (i.e., KPS, AIBN, and V-50) with constant initial concentrations of 9.3 wt% and 1.5 mM, respectively. Note that we used KPS when we changed the type of surfactant, while SDS was used in the experiments in which the initiator type was changed. Other polymerization conditions were the same in all this group of experiments (see Table 2 for experimental design).

Note that we were not successful to produce nano-particles/stable latexes neither with CTAB nor DTAB; instead we observed precipitations in most of the cases. This negative effect was most probably due to electrostatic interactions between the surfactant and initiator molecules. Note that CTAB and DTAB are positively charged due to ammonium, which attracted electrostatically the free negative ions of KPS and formed a layer on the surfaces of the micelles which reduced the effectiveness of the initiator and neutralized surface charges of the forming micelles/particles that caused stability lost and therefore resulted. Similar electrostatic attractions and their negative effects were also reported in earlier studies in which DTAB and AOT (sodium bis(2-ethylexylsulfosuccinate)) were used for the emulsion polymerization of MMA [31].

In contrast, we were able to produce magnetic polymeric nano-particles and their stable latexes when we used a negatively charged surfactant, i.e., SDS. Most probably, there was no adsorption of the initiator molecules on the micelles; KPS radicals stayed in aqueous phase and successfully initiated emulsion polymerizations at high surfactant to monomer ratio. Considering these results, we decided to use SDS as surfactant in the rest of the experiments discussed below.

Three different initiators, two water-soluble hydrophilic (i.e., KPS and V-50) and organic phase-soluble more hydrophobic (i.e., AIBN) were used as initiator as in the emulsion polymerization at high surfactant to monomer ratio. Note that SDS was the surfactant in all of these experiments. Table 5 gives the nano-particle size and its distribution obtained using different types of initiators. The smallest size and the narrowest size distribution, and also more stable latexes were obtained with KPS, as also mentioned in similar experiments [2].

Table 5 Effects of initiator type on the particle size and size distribution of magnetic poly(MMA/AAc-90/10) copolymeric particles

Experiment no.		Average particle size (nm)	Particle size distribution (PDI)
Initiator type			
P4	**KPS**	125.2	0.193
P5	**AIBN**	150.0	0.218
P6	**V-50**	148.8	0.273
KPS concentration (mM)			
P7	**1.5**	151.9	0.217
P8	**2.0**	130.1	0.195
P9	**2.5**	125.2	0.183

For this reason, in this study KPS is selected as the initiator and used in the rest of the polymerization recipe.

Effects of initiator (KPS) concentration

We performed a series of emulsion polymerization at high surfactant to monomer ratio with the selected initiator (i.e., KPS) by changing its concentration. In this group of experiments, we used KPS with three different concentrations (1.5, 2.0, and 2.5 mM) in the feed and produced magnetic poly(MMA/AAc-90/10) copolymeric particles were prepared to investigate the effect of KPS concentration on the particle size and size distribution. Table 5 indicates that the higher initiator concentration results in a decrease in the particle size. Note that KPS is a water-soluble initiator. When its concentration is high the initiator (KPS) molecules diffuse within the dispersion phase (i.e., water) faster and find the micelles swollen with monomer (typical in microemulsions) and or magnetite particles carrying monomer on their surfaces (most probably), and start polymerization in more points which leads smaller particles, as also reported by Macias et al. [31]. Xie and coworkers have also prepared magnetic poly(St-BA-MMA) nanoparticles with different concentrations of KPS [12]. They reported that an increase in the KPS content may lead to a higher number of primary particles, and therefore smaller particle size are achieved, however, the increase in the electrolyte concentration in the polymerization system may depress the electrical double layer of the primary particle surface which may cause an increase in the particle size. When one of these two factors was predominant over the other one, the particles were bigger or smaller. Increasing the ionic strength (due to increase in the KPS concentration) may cause a decrease in the Debye length which might cause coagulation or coalescence process as the particles can approach close. In our case, since we have not seen any coagulation (neither microscopically nor by Zeta Sizer), most probably increasing KPS concentration leads to the formation of higher number of primary particles and also the number of polymeric particles containing no magnetite particles, as a result, smaller particle sizes were observed.

Effects of magnetite (Fe_3O_4)/monomer ratio

As mentioned in the related literature, the ratio of magnetite (the seed particles) to the monomer used in the feed is one of the most important parameters which are effective not only on the size and distribution but also on the quality (sphericity and mono dispersity) of the latex particles synthesized and the product (latex) stability [8, 9, 25, 32]. For instance, Kondo and Fukuda prepared magnetic poly(St/NIPAM/MAA) latex particles using two-step emulsifier-free emulsion polymerization and reported that the hydrodynamic diameter of the magnetic latex particles decreased with increasing weight ratio of magnetite to monomers [32].

In this group of studies, we copolymerized MMA and AAc in the media containing different amounts of magnetite and comonomers. The weight percentage of magnetite (considering only amounts of magnetite and total monomers), which is the so-called ''magnetite/monomer ratio'', was 5%, 25%, and 50%. As seen here, the average particle size and size distribution decreased from 136.5 nm to 120.9 nm and from 0.3 to 0.183, respectively, when we increased the weight ratio of magnetite/monomer from 5 to 50 (Table 6), which were considerable changes. This is expected, because when the magnetite content is increased there will be more seed particles in the reaction medium, if we assumed that polymerization will occur homogeneously (evenly) throughout the reaction vessel, each particles will get less amount of polymer (means thinner polymer coating), and therefore particles with smaller sizes will be formed. Note that we did attempt to use less magnetite (less than 5%) or more (more than 50%) in the preliminary experiments. However, in the first case the copolymeric particles were not magnetic (not observable magnetism), and in the later case aggregation and incomplete polymer coatings were observed.

Table 6 Effects of several parameters on the particle size and size distribution of magnetic poly(MMA/AAc-90/10) copolymeric particles

Experiment no.		Average particle size (nm)	Particle size distribution (PDI)
Magnetite (Fe_3O_4) /monomer ratio (wt%)			
P10	**5**	136.5	0.300
P11	**25**	125.2	0.183
P12	**50**	120.9	0.158
KPS concentration (mM)			
P13	**1.11**	159.7	0.251
P14	**1.47**	125.2	0.183
P15	**2.94**	117.5	0.206

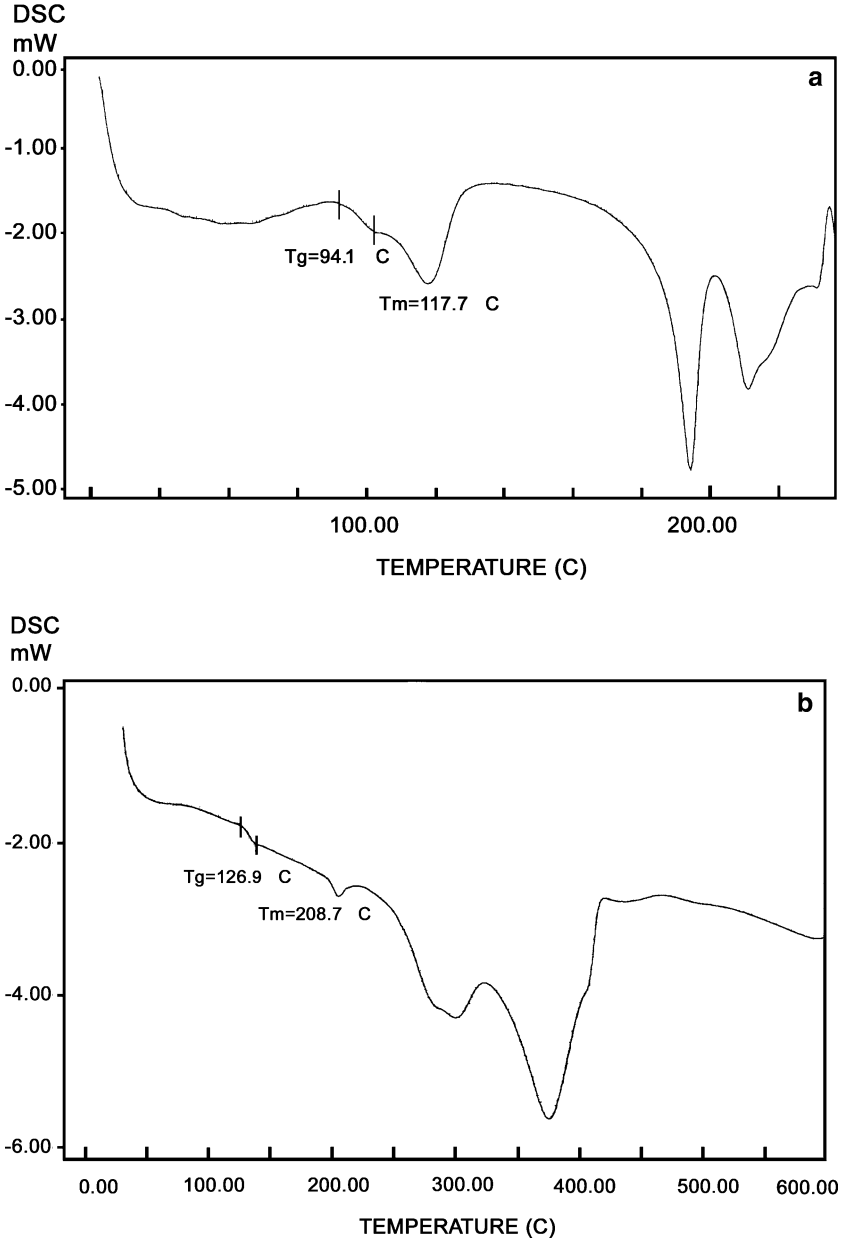

Fig. 2 Representative DSC thermograms: (**a**) plain nanoparticles and (**b**) magnetic nanoparticles (containing 25% Fe_3O_4)

Effects of surfactant (SDS)/monomer ratio

Note that the surfactant (SDS) concentration, especially the ratio of SDS/monomer is a very important parameter in general in emulsion polymerization. It was reported that if the SDS/monomer mass ratio is lower than about 1.0, the polymerization shifts from micro-emulsion to mini-emulsion or even to classical emulsion limits (at lower values). It is also recommended that in order to obtain stable latexes the SDS/monomer ratio in micro-emulsion formulation should be around 1.0–3.0 [33–35]. Note that this is still quite high. High concentrations of SDS mean pollution of latexes which may cause problems in further applications. Since we have seed magnetite nano-particles in the feed, we decided to use lesser amounts of SDS (in the range of 1.1–2.94 wt/wt).

The effects of surfactant (SDS)/monomer mass ratio on the particle size and the PDI of the nano-particles are given in Table 6. Particle diameters and the PDI of these polymer latexes were in the range of 117.5–159.7 nm (P13, P14, and P15) and 0.183–0.251, respectively. As expected that the average size of the nano-particles decreased with increasing SDS concentration, which is similar to those reported by Xie for the magnetic poly(St/BA/MAA) nano-particles [12]. More SDS means more micelles/particle are supported by the surfactant molecules which leads smaller particles and also more stable latexes due to surface-adsorbed SDS molecules that cause electrostatic repulsion between the latex particles.

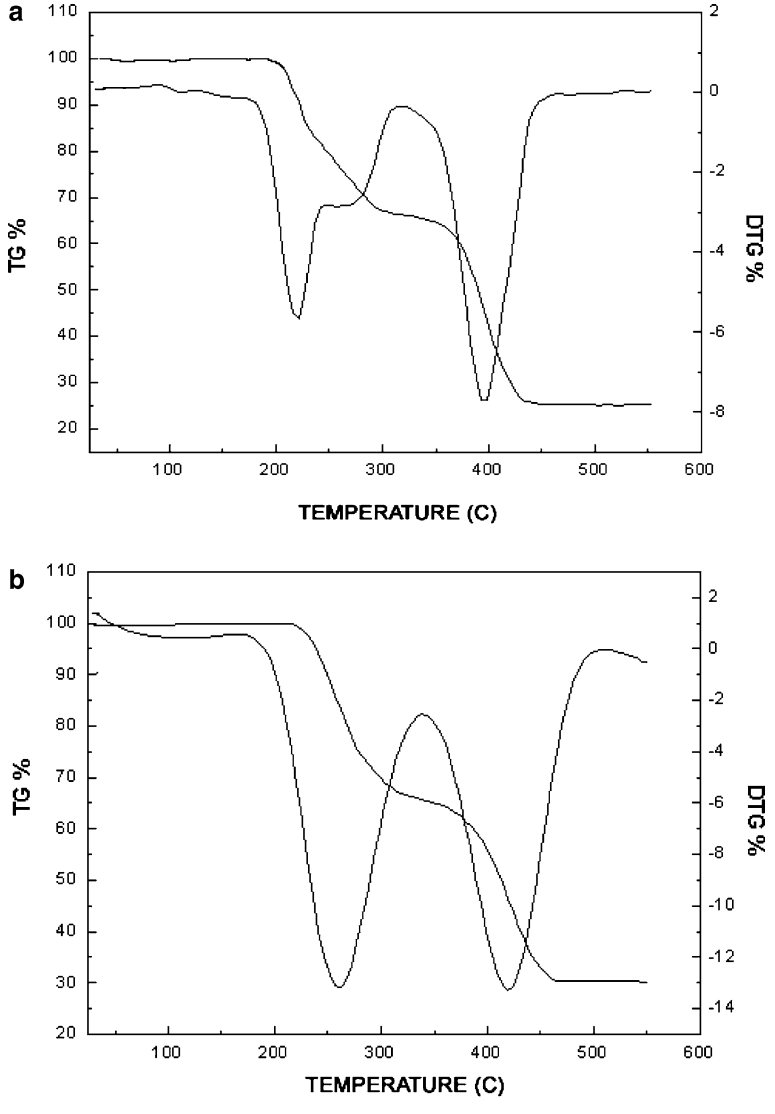

Fig. 3 Representative TGA thermograms: (**a**) plain nano-particles and (**b**) magnetic nano-particles (containing 25% Fe_3O_4)

Properties of magnetic polymeric nano-particles

FTIR spectra of poly(MMA/AAc-90/10) copolymeric nano-particles produced both without using (“plain” or “nonmagnetic polymeric nano-particles”) and with using magnetite seed particles (“magnetic polymeric nano-particles”) were taken. Both spectra were very similar and the following peaks were identified: at 3,550 cm^{-1} OH stretching in carboxylic acid groups, at 2,853–2,922 cm^{-1} CH stretching in CH_2 and CH_3 groups, at 1,736 cm^{-1} C=O stretching in carbonyl groups, at 1,466 cm^{-1} CH_2 bending vibration, at 1,392 cm^{-1} CH_3 bending vibration, at 1,223–1,080 cm^{-1} C–O–C vibration in ester groups, at 991 cm^{-1} C–C stretching of main chain, at 845 cm^{-1} CH out of plain deformation, at 756 cm^{-1} CH_2 rocking. There was only one new signal at 671 cm^{-1} , specific for the stretching vibration of Fe–O groups from the magnetite nano-particles, which confirmed the coating on the magnetite seed particles with copolymer (note that we have separated nonmagnetic and magnetic polymeric particles effectively), as also reported in the related literature [1, 27] .

Thermal properties and behavior of the plain and magnetic copolymeric nano-particles were examined by DSC and TGA. Representative DSC and TGA thermograms are given in Figs. 2 and 3, respectively. The glass transition (T_g), melting temperature (T_m), and decomposition temperatures (T_{decom}) for both nano-particles are given in Table 7. As seen here, there are very significant increases in the T_g, T_m, and T_{decom} values when magnetite particles incorporated within the copolymeric nano-particles as also reported by Deng et al. [10]. The decomposition temperatures obtained with TGA were both higher and the temperature ranges were wider comparing those obtained with DSC. However, in both cases, thermal stability increases were very profound. Most probably, polymerization on magnetite aggregates and it did cause formation of different structures at molecular level (different entanglement, crystallinity, and even may be orientation), which in turn, resulted those changes. In general, sense may be important in the application of these nano-particles at

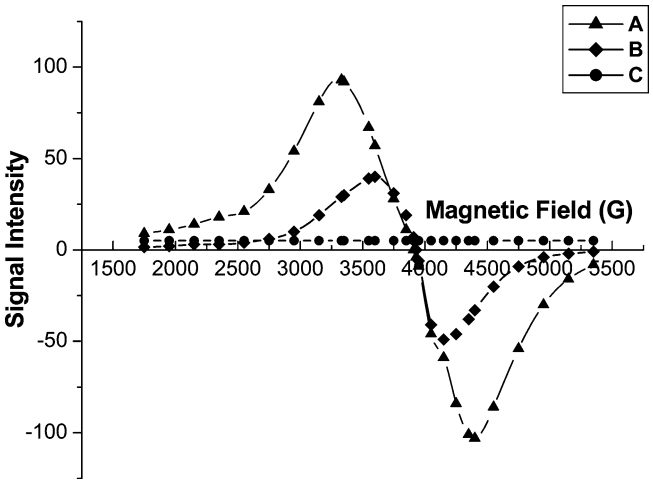

Fig. 4 Representative ESR spectra: (**a**) magnetite nano-particles (Fe_3O_4); (**b**) magnetic polymeric nano-particles (containing 25% Fe_3O_4); and (**c**) plain polymeric nano-particles

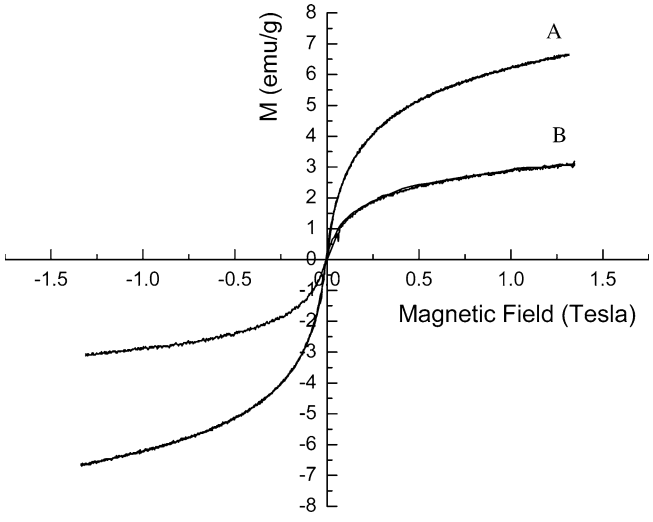

Fig. 5 Representative magnetization curves: (**a**) magnetite nano-particles (Fe_3O_4); (**b**) magnetic nano-particles (containing 25% Fe_3O_4)

Table 7 Thermal properties of plain and magnetic poly(MMA/AAc-90/10) copolymeric nano-particles

T_g (°C)	T_m (°C)	T_{decom} (°C)[a]
Plain poly(MMA/AAc-90/10) copolymeric nano-particles		
94.1	117.7	195–210 (225–395)
Magnetic poly(MMA/AAc-90/10) copolymeric nano-particles		
126.9	208.7	300–375 (235–410)[b] (260–425)[c]

[a]The values in the parentheses were found from TGA thermograms.
[b]The values for the nano-particles containing 15% magnetite.
[c]The values for the nano-particles containing 25% magnetite.

elevated temperatures. The TGA results also show that the increase in the magnetite content further improves the thermal stability of the nanoparticles. The magnetic copolymers containing 15 and 25% Fe_3O_4 particles were decomposed at 235–410 and 260–425 °C, respectively. As seen in the TGA thermographs (Fig. 3), decomposition occurs in two steps. Up to 600 °C, the mass loss of plain copolymeric nano-particles is 75%, while it is 72% and 66% for magnetic nano-particles containing 15% and 25% Fe_3O_4, respectively.

The presence of magnetite particles in the copolymeric nano-particles was confirmed by ESR. Representative ESR spectra of the plain copolymeric nano-particles, magnetic copolymeric nano-particles, and magnetite (Fe_3O_4) particles are given in Fig. 4. As seen here, magnetite particles alone typically show intensity of 100 around 3,300 G applied magnetic field, while relative intensity of the magnetic copolymeric nano-particles decreases to about 45 at the maximum which shifts to around 3,800 G due to the effects of the polymeric coating on the magnetite seed particles. Note also that the plain poly(MMA/AAc) copolymer nano-particles do not exhibit any magnetic property, as expected.

The magnetic properties of magnetic polymeric particles were also studied by using a vibrating-sample magnetometer. Here, applied magnetic field (tesla) was changed and magnetization (M, emu g^{-1}) was measured. A representative magnetization curves for magnetite nano-particles (Fe_3O_4) and magnetic copolymeric nano-particles are shown in Fig. 5. Note that both the magnetite and the magnetic copolymeric nano-particles were super-paramagnetic and no remanence was observed when the magnetic field is removed. The saturation magnetizations obtained for magnetite and magnetic copolymeric nano-particles are 6.601 and 3.190 emu g^{-1}, respectively.

Conclusions

Super paramagnetic poly(MMA/AAc-90/10) nano-particles were synthesized in situ via two steps: (1) preparation of magnetite (Fe_3O_4) nano-particles by co-precipitation method and (2) emulsion polymerization at high surfactant/monomer ratio of MMA and AAc monomers in the presence Fe_3O_4 nano-particles. Studies on particle size and size distribution of the magnetite nano-particles revealed that the change in Fe^{2+}/Fe^{3+} molar ratio, stirring rate, and pH plays an important role in controlling the particle size and magnetic property. On the other hand, the concentration of NaOH and temperature does not affect the size significantly. The smallest size obtained was 40.9 nm. Conventional emulsion polymerization at high surfactant/monomer ratio technique was used for the coating of the magnetite nano-particles with this size. The results showed that SDS and KPS are the most convenient surface active agent and initiator for this system. Depending on the reaction parameters the size range obtained was between 115 and 300 nm for the polymer-coated nano-particles. Increasing magnetite, surfactant content, and KPS concentration decreased the particle size. Zeta potential of the smallest particle was −20.1 mV, which indicates the carboxylic acid groups on the particle surfaces. These magnetically loaded polymeric nano-particles did not loose their magnetic property after the coating. They still showed super-paramagnetic property. Applications of these novel magnetically loaded polymeric nano-particles for diverse biomedical applications including electrochemical-based DNA sensors and separation/purification of stem cells are under investigation.

Acknowledgement Prof. Erhan Piskin was supported by Turkish Academy of Sciences as a full member.

References

1. Yamaura M, Camilo RL, Sampaio LC, Macedo MA, Nakamura M, Toma HE (2004) J Magn Magn Mater 279:210–217
2. Ramirez LP, Landfester K (2003) Macromol Chem Phys 204:22–31
3. Šafařík I, Šafaříková M (2002) Monatsh Chem 133:737–759
4. Brigger I, Durernet C, Couvreur P (2002) Adv Drug Deliv Rev 54:631–651
5. Harma H (2002) Technol Rev 126:1–25
6. Deng Y, Wang L, Yang W, Fu S, Elaïssari A (2003) J Magn Magn Mater 257(1):69–78
7. Dresco PA, Zaitsev VS, Gambino RJ, Chu B (1999) Langmuir 15:1945–1951
8. Xu ZZ, Wang CC, Yang WL, Deng YH, Fu SK (2004) J Magn Magn Mater 277:136–143
9. Arias JL, Gallardo V, Gómez-Lopera SA, Plaza RC, Delgado AV (2001) J Controlled Release 77:309–321
10. Deng J, Peng Y, He C, Long X, Li P, Chan ASC (2003) Polym Int 52:1182–1187
11. Wormuth K (2001) J Colloid Interface Sci 241:366–377
12. Xie G, Zhang Q, Luo Z, Wu M, Li T(2003) J Appl Polym Sci 87:1733–1738
13. Zaitsev VS, Filimonov DS, Presnyakov IA, Gambino RJ, Chu B (1999) J Colloid Interface Sci 212:49–57
14. Babes L, Denizot B, Tanguy G, Jeune JJL, Jallet P (1999) J Colloid Interface Sci 212(2):474–482
15. Zhu Y, Wu Q (1999) J Nanopart Res 1:393–396
16. Massart R (1981) IEEE Trans Magn Mag 17:1247
17. Khalafalla SE, Reimers GW (1980) IEEE Trans Magn Mag 16:178
18. Pardoe H, Chua-anusorn W, St Pierre TG, Dobson J (2001) J Magn Magn Mater 225:41
19. Morais PC, Garg VK, Oliveira AC, Silva LP, Azevedo RB, Silva AML, Lima ECD (2001) J Magn Magn Mater 225:37–40

20. Gribanov NM, Bibik EE, Buzunov OV, Naumov VN (1990) J Magn Magn Mater 85:7
21. Liu ZL, Liu YJ, Yao KL, Ding ZH, Tao J, Wang X (2002) J Mater Synth Process 10:2
22. Kim DK, Zhang Y, Voit W, Rao KV, Muhammed M (2001) J Magn Magn Mater 225:30–36
23. Babes L, Denizot B, Tanguy G, Le Jeune JJ, Jallet P (1999) J Colloid Interface Sci 212:474
24. Jiang W, Yang HC, Yang SY, Horng HE, Hung JC, Chen YC, Hong CY (2004) J Magn Magn Mater (in press)
25. Horák D, Semenyuk N, Lednický F (2003) J Polym Sci Part A: Polym Chem 41:1848–1863
26. Cornell RM, Schertmann U (1991) Iron oxides in the laboratory; preparation and characterization. VCH Publishers, Weinheim
27. Bocanegra-Diaz A, Mohallem NDS, Sinisterra RD (2003) J Braz Chem Soc 14:936–941
28. Montagne F, Monval-Mondain O, Pichot C, Mozzanega H, Elaïssari A (2002) J Magn Magn Mater 250:302–312
29. Cornell RM, Schertmann U (1996) The iron oxides; structure, properties, reactions, occurrence and uses. VCH Publishers, Weinheim
30. Özer F, Beşkardeş MO, Zareie H, Pişkin E (2000) J Appl Polym Sci 82:237–242
31. Macias ER, Rodríguez-Guadarrama LA, Cisneros BA, Castañeda A, Mendizábal E, Puig JE (1995) Colloids Surf A: Physicochem Eng Aspects 103:119–126
32. Kondo A, Fukuda H (1999) Colloids Surf A: Physiochem Eng Aspects 153:435–438
33. David G, Özer F, Simionescu BC, Zareie H, Pişkin E (2002) Eur Polym J 38:73–78
34. Yildiz U, Capek I (2003) Polymer 44:2193–2200
35. Babaç C, Guven G, David G, Simionescu BC, Pişkin E (2004) Eur Polym J 40(8):1947–1952